AD870867

ANU-P/964
January 1987

Accepted for publication in Nuclear Physics A

REORIENTATION EFFECTS FOR 52 MeV VECTOR POLARIZED DEUTERONS

J. Nurzynski
Department of Nuclear Physics, Research School
of Physical Sciences, The Australian National University,
GPO Box 4, Canberra, ACT 2601, Australia

T. Kihm, K.T. Knöpfle and G. Mairle
Max-Planck-Institut für Kernphysik,
D-6900 Heidelberg, W.Germany

H. Clement
Physikalisches Institut der Universität Tübingen,
Morgenstelle, D-7400 Tübingen, W.Germany

Abstract: The differential cross sections, $d\sigma(\theta)/d\Omega$, and the vector analysing powers, $iT_{11}(\theta)$, were measured for the elastic and inelastic scattering of 52 MeV vector polarized deuterons from ^{20}Ne, ^{22}Ne, ^{26}Mg, ^{28}Si, ^{32}S, ^{34}S, ^{36}Ar and ^{40}Ar nuclei. Coupled channels analysis was carried out using an axially symmetric rotational model with either prolate or oblate quadrupole deformations for each isotope. Calculations assuming harmonic vibrator model were also carried out. In general, reorientation effects were found to be weak. A global optical model potential containing an imaginary spin-orbit component was found to be the most suitable in describing the experimental data at this energy.

NUCLEAR REACTIONS ^{20,22}Ne, ^{26}Mg, ^{28}Si, ^{32,34}S, ^{36,40}Ar($\vec{d}$,d), ($\vec{d}$,d'), E = 52 MeV; measured $d\sigma(\theta)/d\Omega$ and $iT_{11}(\theta)$; coupled channels analysis; deduced β_2 and optical model parameters. ^{28}Si, ^{32}S and ^{40}Ar natural targets; ^{20,22}Ne, ^{26}Mg, ^{34}S and ^{36}Ar enriched targets.

1. Introduction

It has been pointed out that reorientation of electric quadrupole moment for the 2^+ states may play an important role in scattering[1,2]) of protons and deuterons. For deformed nuclei the 2^+-2^+ matrix element, which is proportional to the quadrupole moment, Q_{2^+}, may have a sufficiently strong influence on the analysing powers to allow to distinguish between prolate and oblate shapes of the target nuclei. The effect is energy dependent and is expected to be stronger at lower projectile energies. However, due to contributions from indirect processes, such as energy fluctuations and resonance scattering, interpretation of the low energy data may be difficult. More recently it was reported that reorientation effects may be significant at such high energies as 65 MeV for protons and 56 MeV for deuterons[3]).

So far no systematic study of reorientation effects in scattering of polarized particles has been undertaken. However, from the available results, confined mainly to energies below 25 MeV, certain patterns can be noticed. In nearly all cases the reorientation process is found to affect relatively strongly the analysing powers for scattering to the first, 2^+_1, excited states in even-even nuclei and to a certain extent also the inelastic scattering differential cross sections. Scattering to the second, 2^+_2, states is influenced less strongly[4]). For the oscillating analysing powers the reorientation process shifts the oscillations to smaller angles and damps the oscillation amplitude for prolate quadrupole deformations. For oblate shapes the effect is the opposite; the oscillations are shifted towards larger angles and their amplitude is increased. Such behaviour was demonstrated for 24.5 MeV protons scattered from ^{152}Sm [ref.[1])], 9.4 MeV deuterons scattered from ^{28}Si [ref [5])], 20.5 MeV deuterons scattered from ^{154}Sm [ref.[6])], 20 MeV deuterons scattered from ^{24}Mg, ^{28}Si and ^{54}Cr [ref.[4])]

and 18 MeV deuterons scattered from ^{32}S [ref.^{4})].

It should be noted that for ^{32}S reorientation effects were also studied using energy averaged results corresponding to deuteron incident energy E_d = 9.7 MeV [ref.^{5})]. At this energy, experimental data could not be fitted using either prolate or oblate shapes for ^{32}S. Good agreement between theory and experiment was, however, obtained assuming the harmonic vibration model. On the other hand, at E_d = 18 MeV, distinction between oblate and prolate shapes for ^{32}S is clear with a prolate quadrupole deformation giving definitely a better description of the experimental results. Thus one set of data describes ^{32}S as a harmonic vibrator while the other shows it to be deformed with a prolate shape. It is clear, therefore, that even in cases for which agreement between theory and experiment is good discrimination between nuclear shapes and models should be taken with caution.

At very low energies, ≤10 MeV, strong dependence on the sign of the quadrupole deformation parameter, β_2, was found not only for the inelastic but also for the elastic scattering [5]). At these energies experimental results had to be averaged over a range of incident energies in order to minimise effects of resonance scattering.

Less clear reorientation effects were reported for 20.3 MeV protons scattered from ^{28}Si [ref.^{7})], 12.3 MeV deuterons scattered from $^{54,56,58}Fe$ [ref.^{8})], 10 MeV deuterons scattered from ^{24}Mg [ref.^{5})] and 15 MeV deuterons scattered from ^{56}Fe [ref.^{2})]. For 20.3 MeV protons and for 10 MeV and 15 MeV deuterons, coupled channels calculations predict strong dependence of the analysing powers on the sign of β_2. However, agreement between theory and experiment is far from satisfactory. At 12.3 MeV deuteron energy theoretical predictions for prolate and oblate shapes are shown only for ^{56}Fe. For this nucleus fits to the elastic scattering favour an <u>oblate</u>

deformation while the distributions for the 2_1^+ inelastic scattering are described better assuming a prolate shape.

At higher energies, a small but clear angular shift was reported for 65 MeV protons scattered from ^{24}Mg [ref.^{3})]. The displayed fit to the analysing powers for the 2_1^+ state is exceptionally good for a prolate shape. However, fits to other anuglar distributions are not shown. A more extensive coupled channels analysis was carried out later for 65 protons scattered from ^{24}Mg, ^{28}Si and ^{32}S [ref.^{9})]. Results of this analysis indicated that good fits could be obtained only for the elastic scattering. Fits for the inelastic scattering, and in particular for the 2_1^+ analysing powers, are far from satisfactory. The discrepency between theory and experiment is particularly strong for the 2_1^+ state in ^{24}Mg. These calculations put in doubt the earlier results of ref.^{3}).

An attempt to distinguish between prolate and oblate shapes was also made for 65 MeV protons scattered from ^{28}Si [ref.^{10})]. However, the predicted small angular shift for the two shapes and the poor quality of fits make the results inconclusive.

For the 56 MeV deuterons reorientation effects were reported for ^{24}Mg and ^{28}Si [ref.^{3})]. At this energy the anguiar dependence of the vector analysing powers $iT_{11}(\theta)$ for the 2_1^+ states is distinctly different from that observed at lower energies. The region sensitive to the sign of β_2 was found to be confined to angles between about 20° and 60°. By comparing coupled channels calculations with the experimental data it was possible tc distinguish between prolate and oblate shapes with more clear discrimination being for ^{28}Si. However, here again, theoretical predictions for the two signs of β_2 are shown only for the $iT_{11}(\theta)$ distributions for the 2_1^+ states.

The aim of the work described in this paper was to explore more systematically this higher energy region for the s-d shell nuclei. The experimental procedure is described in section 2. Section 3 contains details of the coupled channels analysis. Discussion and conclusions are presented in section 4.

2. Experimental procedure and results

The measurements described here were performed using 52 MeV vector polarized deuterons supplied by the Lamb-shift polarized ion source[11]) and by the Karlsruhe isochronous cyclotron. The beam transport system was set in an achromatic mode delivering about 5 nA of polarized deuteron beam on target with an overall energy resolution of detected deuterons of about 270 keV being mainly due to the beam resolution. The following targets were used in the measurements: ^{20}Ne (99.9% enriched), ^{22}Ne (99.7% enriched), ^{26}Mg(99.7% enriched), Si(92.2% of ^{28}Si), S(SH_2 with 95% of $^{32}SH_2$), ^{34}S($^{34}SH_2$, 89.8% enriched), ^{36}Ar(99.5% enriched) and Ar(99.59% of ^{40}Ar). Meausurements of the differential cross sections, $d\sigma(\Theta)/d\Omega$, and of the vector analysing powers, $iT_{11}(\Theta)$, for the elastic and inelastic deuteron scattering were carried out in the range of angles of about 10° - 80° (lab), in steps of 1.5° for up to about 50° and in steps of 3° for larger angles. The method of measurement of the vector analysing powers using cyclotrons is described in ref.[12]). The detector system consisted of six ΔE-E solid state counter telescopes placed at symmetric angles with respect to the beam direction. The detectors were mounted on two remotely controlled, moveable tables inside a large scattering chamber. The angular distance between the adjacent detector telescopes on each table was 3° and the angular resolution of the detector slit systems was $\pm 0.5^\circ$. The thickness of the detectors was 1500 μm or 2000 μm for the ΔE detectors and 7000μm (2000μm + 5000μm) for the

E detectors. The usual pulse multiplication method was used for the particle identification. During the measurements the beam polarization was flipped every few minutes according to a preset value of the beam current integration counts.

The absolute value of the beam polarization was monitored using the $^{12}C(\vec{d},d)^{12}C$ elastic scattering at $\Theta = 47°$(lab). This angle corresponds to an optimum value of the $[iT_{11}(\Theta)]^2 d\sigma(\Theta)/d\Omega$ parameter with the analysing power $iT_{11}(47°) = 0.318 \pm 0.035$ being known from the double scattering measurements[13]). The beam polarimeter was mounted downstream, outside the main scattering chamber and it was followed by a Faraday cup used in the measurements of the integrated charge. The target of the beam polarimeter consisted of a large polyethylene foil. Scattered deuterons were detected by two NaI(Tℓ) detectors placed symmetrically in respect of the deuteron beam. The thickness of the NaI(Tℓ) crystals was chosen in such a way as to allow a clear separation of deuterons from the high energy protons from the $^{12}C(d,p)^{13}C$ reaction. In addition, a thin Al foil was also mounted in front of each crystal to suppress $Z \geq 2$ particles. The average beam polarization, p_z, during the measurements was $0.46 \pm 0.0.05$ and its stability was within about 2% over a long period of data collection.

Deuteron spectra from the main detectors and from the beam monitor were stored on magnetic tapes and were analysed off-line using an MPI VAX-780 computer system. All data reduction calculations were carried out using computer code LORNA[14]). Written for the 52 MeV data, the code can have a more general application. It performs a global analysis of particle spectra and it was written in such a way as to make it simple to use and to allow for an easy interaction of the user with the calculations. Typically about 200 spectra were taken for each target. Program LORNA converted them to $d\sigma(\Theta)/d\Omega$ and to $iT_{11}(\Theta)$ angular distributions in about 1.5 minutes for each

excitation energy. Calculations of the errors of the experimental data include statistical uncertainties, background subtraction and beam polarization errors.

All experimental distributions are shown together with the theoretical predictions in the next section. However, as mentioned earlier, the $iT_{11}(\Theta)$ analysing powers for the 2_1^+ states are expected to carry relatively strong dependence on the sign of β_2. It is, therefore, also interesting to compare the relevant experimental results separately in one figure. Figure 1 shows that except for one isotope, ^{28}Si, all $iT_{11}(\Theta)$ distributions for the 2_1^+ states display similar features. These results will be discussed further in section 4.

3. Theoretical analysis

The coupled channels analysis of the experimental data was carried out using code ECIS[15]). All theoretical calculations were performed using the Australian National University UNIVAC 1100/82 computer. For each target isotope four distributions, $d\sigma(\Theta)/d\Omega$ and $iT_{11}(\Theta)$ for the ground and for the first 2_1^+ excited states, were fitted simultaneously. In order to see whether theoretical fits are sensitive to the sign of the quadrupole deformation, independent searches of potential parameters were carried out using either positive or negative β_2 parameter for each target isotope. In all these calculations an axially symmetric rotational model containing quadrupole and hexadecapole deformations was assumed for all nuclei. The central and the spin-orbit components of the deuteron-nucleus interaction potential were deformed and the same deformation parameters were used for all of them.

The optical model parameter search was first carried out using, as starting values, potential parameters derived earlier [16]) for the 52 MeV deuteron elastic scattering. Unfortunately, searches based on any of the four sets of parameters of ref.[16]) did not result in fitting simultaneously the distributions for the elastic and the inelastic scattering. The potential F' of ref.[17]), containing an imaginary spin-orbit component, was tried next and it was found to give a significantly better description of the experimental results. The potential F' contains five components, defined by a total of 15 parameters. In the initial series of calculations the experimental results for each nucleus and for either positive or negative β_2 were fitted by searching on all 15 parameters in groups of up to 10 parameters at a time and with all 15 parameters varied simultaneously in the final stages of parameter optimization. After finishing the calculations for all nuclei and for both signs of β_2 it was found that, with some exceptions, all 15 parameters fluctuated around certain smoothly varying, mass dependent values. Close examination of all these parameters suggested that many of them could be fixed at their original values and that the 15 parameter search could be reduced to a search on only four parameters. In particular, the analysis involving searches on all 15 parameters indicated (a) that the depth of the central volume absorption potential, W_s, could be constant for all target isotopes but that its value should be reduced to 2.07 MeV; (b) that the radii of the central surface and volume absorption potentials should be different but that the reduced radius of the volume absorption potential, could be fixed at the value r_I as given for potential F'; (c) that all other parameters, except for V_R, a_o, W_D and r_D, could be assumed to have the values given in ref.[17]). In particular, no compelling evidence was found for a need to alter the parameters of the spin-orbit components from their original values.

Taking into account results of the 15 parameters search, as described above, the analysis was repeated by searching on only four parameters, V_R, a_o, W_D and r_D. In general, the resulting fits were found to be similar to those obtained by searching on all 15 parameters. The searching procedure was not only considerably easier and faster but it also eliminated some spurious parameter fluctuations. Results of the four parameter search for each isotope were taken as representing the best theoretical predictions at this deuteron energy. They are displayed in figs 2-5 for $\beta_2 > 0$ and for $\beta_2 < 0$. Except for ^{28}Si, the full and the dotted lines are for the calculations using prolate and oblate deformations, respectively. For ^{28}Si the representation is reversed. The four individually adjusted parameters for each target isotope and for each sign of β_2 parameter, are shown in fig. 6. They were found to be close to their original values which are also shown in the same figure. Deformation parameters, β_2 and β_4, used in the coupled channels calculations are listed in Table 1.

Finally, in order to see to what extent theoretical predictions are model-dependent, the four parameter search was also carried out assuming a harmonic vibrational model for each isotope. Results of the calculations are shown as the dashed lines in figs 2-5 and the corresponding coupling parameters β_{02} are listed also in Table 1. Final parameters V_R, a_o, W_D and R_D were found to be the same as those corresponding to the full lines in figs 2-5.

4. Discussion and conclusions

A survey of the quadrupole moments for nuclei in the s-d shell[18]) indicates that only ^{28}Si nucleus has a strong oblate quadrupole deformation with the adopted value for the quadrupole moment $Q_{2^+} = +16 \pm 3$ efm^2. Two

other candidates for an oblate shape are ^{34}S and ^{36}Ar with the adopted Q_2^+ values being $+4\pm3$ efm^2 and $+11\pm6$ efm^2, respectively. The Q_2^+ value for ^{34}S is better known and it indicates a nearly spherical shape. Another nucleus for which $|Q_2^+|$ is reported to be small is ^{40}Ar ($Q_2^+ = +1\pm4$ efm^2). Nuclei ^{20}Ne, ^{22}Ne, ^{26}Mg and ^{32}S are prolate with various degrees of deformation.

Experimetal survey of the vector analysing powers for the 2_1^+ states in the s-d shell nuclei (see fig. 1) indicates that the general features of the $iT_{11}(\theta)$ distributions are the same for the prolate nuclei and for nuclei with small $|Q_2^+|$ moments. The only distinctly different distribution is for the nucleus with a strong oblate deformation. This survey indicates that reorientation effects at 52 MeV deuteron energy may allow to identify only nuclei with strong oblate shapes; they do not, however, allow to distinguish between prolate, spherical or nearly spherical nuclei.

As far as the coupled channels calculations are concerned we have found that the global potential F' of ref.[17]) gives, in general, satisfactory simultaneous fits to the four angular distributions for each target isotope. Fits to the $iT_{11}(\theta)$ distributions for the 2_1^+ states could be improved at the expense of the fits to the remaining distributions. However conclusions based on such a procedure might not be meaningful. Considering calculations for the $iT_{11}(\theta)$ to the 2_1^+ states, as presented in figs. 2-5, it is clear that the most clear discrimination between prolate and oblate quadrupole shapes is in the case of ^{26}Mg and ^{28}Si nuclei. Fits to $^{20,22}Ne$ are rather poor and agreement between the experimental and the theoretical results is only marginally better for prolate shapes. Experimental results for this pair of isotopes were found to be the most difficult to fit when using the coupled channels procedure. The easiest to fit were the experimental results for $^{32,34}S$ and for $^{36,40}Ar$ isotopes. Figs.4 and 5 show that an assumption of prolate shapes gives only marginally

better representation of the dat. for ^{32,34}S with practically no difference between the two signs of β_2 for ^{36,40}Ar. In general, reorientation effects in the 52 MeV deuteron scattering appear to be weak. This is further confirmed by comparing rotational and vibrational model calculations. The basic difference between the two models is in the 2^+-2^+ matrix elements which vanish for the harmonic vibrator. Results presented in figs 2-5 show that, in general, there are no significant differences between the rotational and the vibrational model calculations. Even for ^{26}Mg and ^{28}Si nuclei, calculations using prolate shapes are similar to those obtained using harmonic vibrator. This is in contrast with the results at lower incident energies where for strongly deformed nuclei, even if fits to the experimental data are poor, differences between rotational and vibrational model calculations are generally significant. At 52 MeV the influence of the 2^+-2^+ matrix element is such that only for large positive quadrupole moments a noticable change in the $iT_{11}(\theta)$ analysing powers for the 2_1^+ may be produced. For small or for prolate deformations general character of the calculated analysing powers is nearly the same.

In summary, our experimental survey alone, supported further by the coupled channels calculations, indicates that, in general, reorientation effects at 52 MeV deuteron energy for the s-d shell nuclei are weak. The experimental $iT_{11}(\theta)$ distributions for nuclei with large prolate and with small deformations are found to have similar features. Only in a single case of a strong oblate deformation, for ^{28}Si, was a distinctly different experimental $iT_{11}(\theta)$ distribution observed for the 2_1^+ excitation and only for two isotopes, ^{26}Mg and ^{28}Si, were distinctly different $iT_{11}(\theta)$ predictions for the two signs of β_2 found for the 2_1^+ states. For ^{20}Ne and ^{22}Ne, an assumption of large oblate deformations did not result in altering significantly the calculated $iT_{11}(\theta)$ distributions for the 2_1^+ states.

However the overall fits to all four distributions for each of these two isotopes appear to favour the correct sign of β_2.

Our search for the best interaction potential indicated that potential F' of ref.[17], containing an imaginary spin-orbit component, is the most suitable in describing the experimental results at 52 MeV. Furthermore, with W_s reduced to 2.07 MeV, only four, out of a total of 15, parameters had to be adjusted, in general only slightly, for each target isotope to optimize the theoretical description of the data.

References

1) A.B. Kurepin, R.M. Lombard and J. Raynal, Phys. Lett. 45B(1973)184.

2) J. Raynal, in Proc. Forth Int. Symp. on Polarization Phenomena in Nuclear Reactions, Zürich, 1975, W. Grüebler and V. König, eds (Birkhäuser Verlag, Basel and Stuttgart, 1976) p.271.

3) K. Hatanaka, M. Nakamura, K. Imai, T. Noro, H. Shimizu, H. Sakamoto, J. Shirai, T. Matsusue and K. Nisimura, Phys. Rev. Lett., 46(1981)15.

4) H. Clement, R. Frick, G. Graw, F. Merz, P. Schiemenz, N. Seichert and Sun Tsu Hsun, Phys. Rev. Lett. 45(1980)599.

5) H. Clement, G. Graw, W. Kretschmer and W. Stack, J. Phys. Soc. Japan Suppl. 44(1978)570.

6) H. Clement, R. Frick, G. Graw, I. Oelrich, H.J. Scheerer, P. Schiemenz, N. Seichert and Sun Tsu Hsun, in Proc. Fifth Int. Symp. on Polarization Phenomena in Nuclear Physics, Santa Fe, NM, 1980, G.G. Ohlsen, R.E. Brown, N. Jarmie, W.W. McNaught and G.M. Hale, eds, AIP Conf. Proc. No. 69 (AIP, New York, 1981) p. 376.

7) A.G. Blair, C. Glashausser, R. de Swiniarski, J. Goudergues, R. Lombard, B. Mayer, J. Thirion and P. Vaganov, Phys. Rev. C1(1970)444.

8) R.C. Brown, A.A. Debenham, J.A.R. Griffith, O. Karban, D.C. Kocher and S. Roman, Nucl. Phys. A208(1973)589.

9) S. Kato, K. Okada, M. Kondo, K. Hosono, T. Saito, N. Matsuoka, K. Hatanaka, T. Noro, S. Nagamachi, H. Shimizu, K. Ogino, Y. Kadota, S. Matsuki and M. Wakai, Phys Rev. C31(1985)1616.

10) M. Nakamura, H. Sakaguchi, K. Imai, K. Hatanaka, A. Goto, T. Noro, F. Ohtani, S. Kobayashi, K. Hosono, M. Kondo, S. Kato, K. Ogino and Y. Kadota, J. Phys. Soc. Japan Suppl. 44(1978)557.

11) V. Bechtold, L. Friedrich, D. Finken, G. Strassner and P. Ziegler, in Proc. Forth Int. Symp. on Polarization Phenomena in Nuclear Reactions, Zürich, 1975, W. Grüebler and V. König, eds (Birkhäuser Verlag, Basel and Stuttgart, 1976)p.849.

12) V. König, W. Grüebler and P.A. Schmelzbach, ibid, p. 895.

13) E. Seibt and C. Weddigen, Nucl. Instr. Meth. 100(1980)61.

14) J. Nurzynski, Comp. Phys. Communications 36(1985)295.

15) J. Raynal, Computing as a Language of Physics (IAEA, Vienna, 1972)p.281.

16) G. Mairle, K.T. Knöpfle, H. Riedesel and G.J. Wagner, Nucl. Phys. A339(1980)61.

17) W.W. Daehnick, J.D. Childs and Z. Vrcelj, Phys. Rev. C21(1980)2253.

18) R.H. Spear, Phys. Rep. 73(1981)369 and references therein.

TABLE 1

Parameters β_2, β_4 and β_{02} used in the coupled channels analysis of the 52 MeV vector polarized deuteron scattering from the s-d shell nuclei.

	^{20}Ne	^{22}Ne	^{24}Mg	^{28}Si	^{32}S	^{34}S	^{36}Ar	^{40}Ar
β_2 [a]	+0.50	+0.37	+0.30	-0.34	+0.27	+0.20	+0.18	+0.17
β_4 [a]	+0.05	+0.05	-0.03	+0.08	-0.20	-0.20	+0.10	+0.10
β_2 [b]	-0 53	-0.44	-0.35	+0.34	-0.33	-0.24	-0.18	-0.20
β_4 [b]	+0.05	+0.05	-0.03	+0.08	-0.20	-0.20	+0.10	+0.10
β_{02} [c]	0.50	0.37	0.30	0.34	0.27	0.20	0.17	0.17

a) Deformation parameters associated with the full lines in figs 2-5 and with the full circles in fig. 6.

b) Deformation parameters associated with the dotted lines in figs 2-5 and with the open circles in fig.6.

c) Coupling parameters associated with the dashed lines in figs 2-5 and with the full circles in fig. 6.

Figure Captions.

Fig. 1. Vector analysing powers, $iT_{11}(\theta)$, for the 2_1^+ states in the s-d shell nuclei measured using 52 MeV vector polarized deuterons.

Fig.2. The experimental results (dots) for the elastic and inelastic scattering of 52 MeV vector polarized deuterons from ^{20}Ne and ^{22}Ne compared with the theoretical calculations. Errors smaller than the size of the experimental points are not shown. The coupled channels calculations for an axially symmetric rotational model, carried out using either prolate or oblate quadrupole deformations are shown in the form of the full and the dotted lines. The dashed lines show the calculations using a harmonic vibration model.

Fig. 3 Results for ^{26}Mg and ^{28}Si. See the caption to fig. 2.

Fig. 4 Results for ^{32}S and ^{34}S. See the caption to fig. 2.

Fig. 5. Results for ^{36}Ar and ^{40}Ar. See the caption for fig. 2.

Fig. 6 The optical model parameters V_R, a_o, W_D and R_D. The full circles correspond to the full lines (a rotational model, $\beta_2<0$ for ^{28}Si and $\beta_2>0$ for all remaining nuclei) and to the dashed lines (a harmonic vibrator model) in figs.2-5. The open circles are for the dotted lines in figs.2-5 (a rotational model with the reversed signs of β_2). The coinciding values are also shown as the full circles. The full lines represent the original global parameter values of potential F' taken from ref.[17].

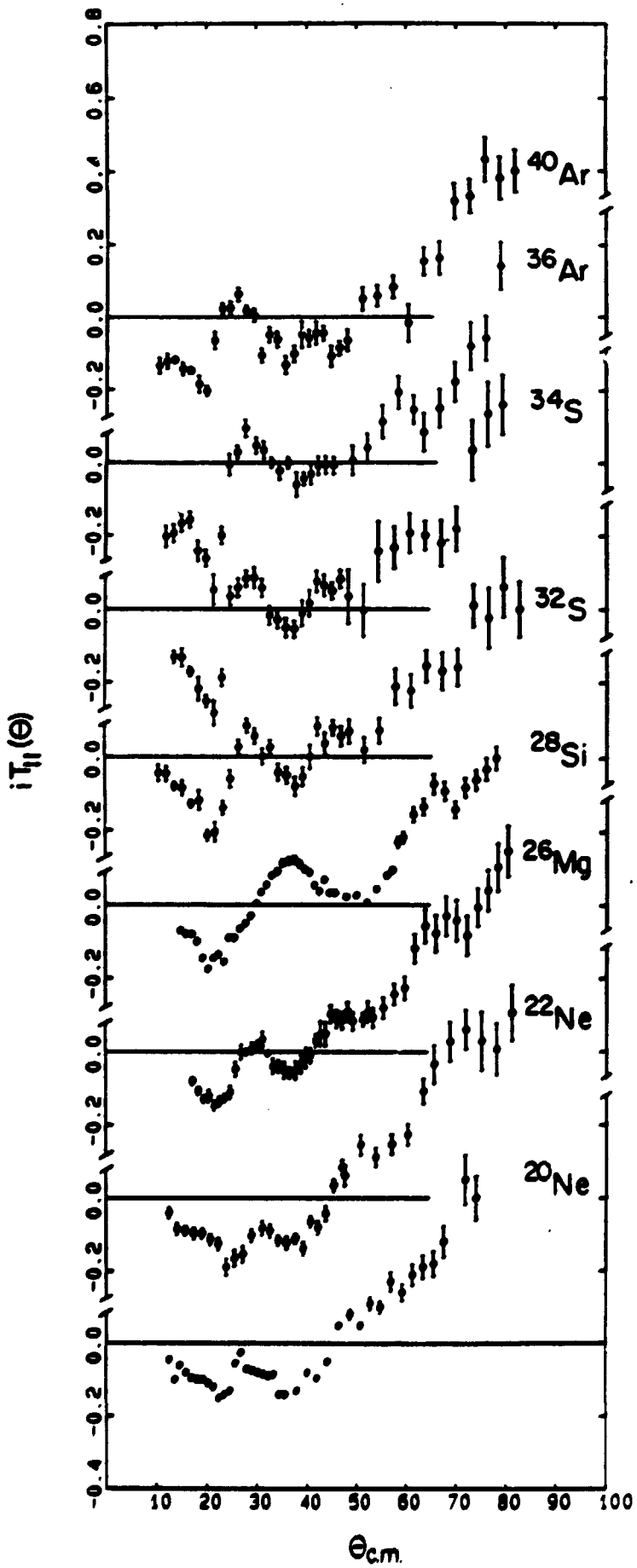
$iT_{11}(\Theta)$
$\Theta_{c.m.}$
^{40}Ar
^{36}Ar
^{34}S
^{32}S
^{28}Si
^{26}Mg
^{22}Ne
^{20}Ne
0.8
0.6
0.4
0.2
0.0
-0.2
-0.4
10
20
30
40
50
60
70
80
90
100

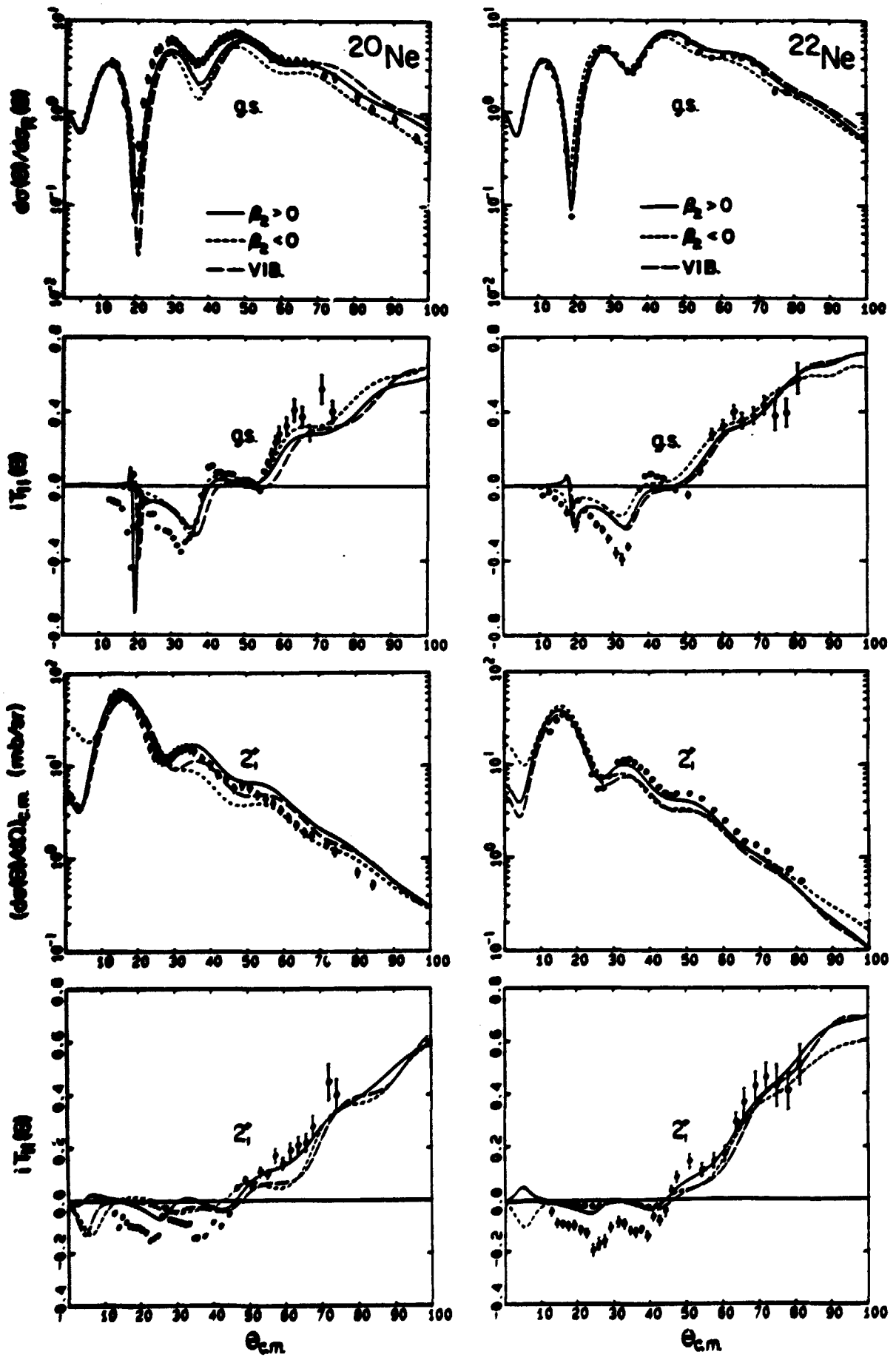
20Ne
22Ne
g.s.
$A_2 > 0$
$A_2 < 0$
VIB.
2_1^+
$\theta_{c.m.}$

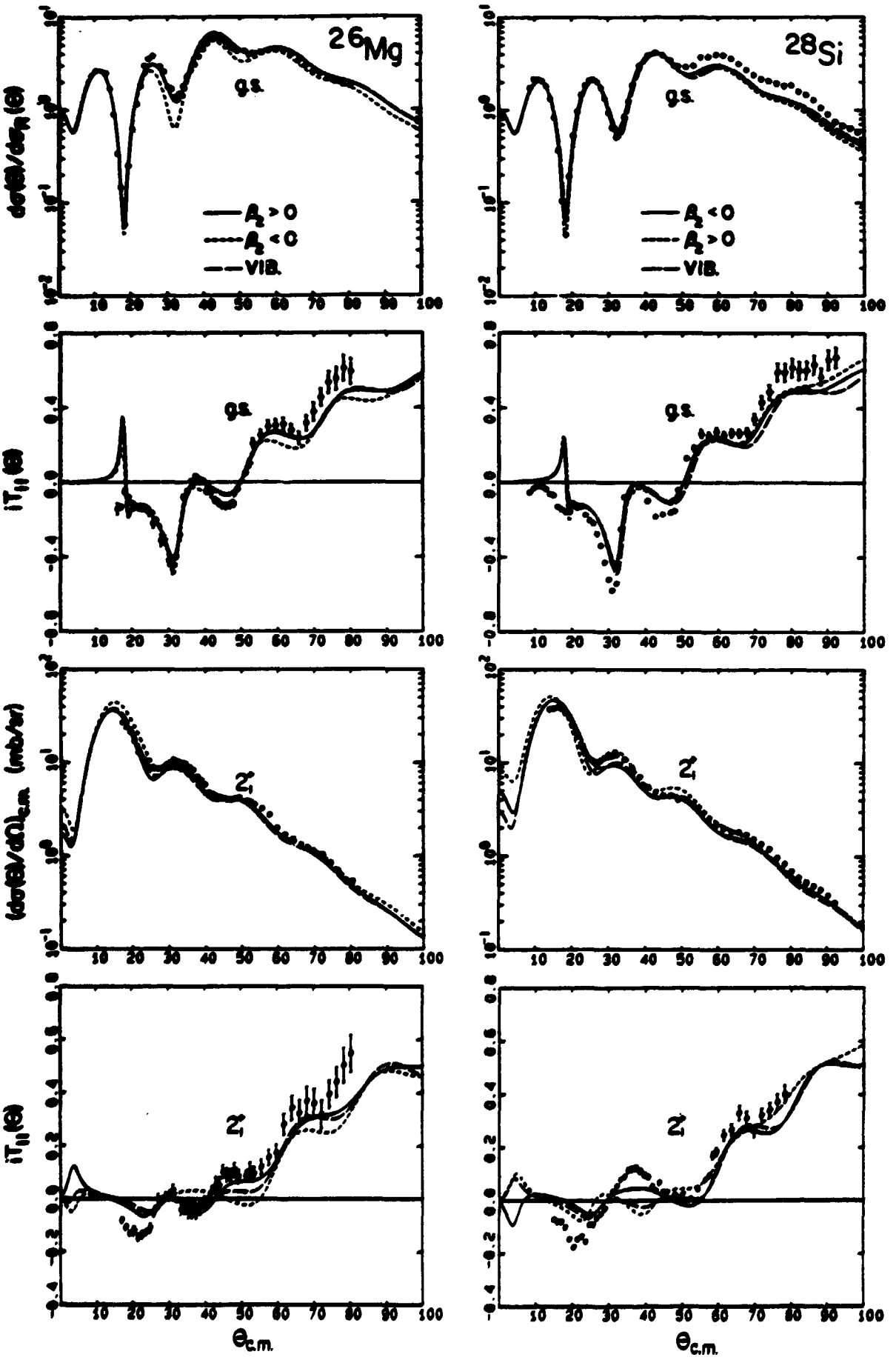
26Mg
28Si
g.s.
2+1
A2 > 0
A2 < 0
VIB.
iT11(θ)
dσ(θ)/dΩ)c.m. (mb/sr)
θc.m.

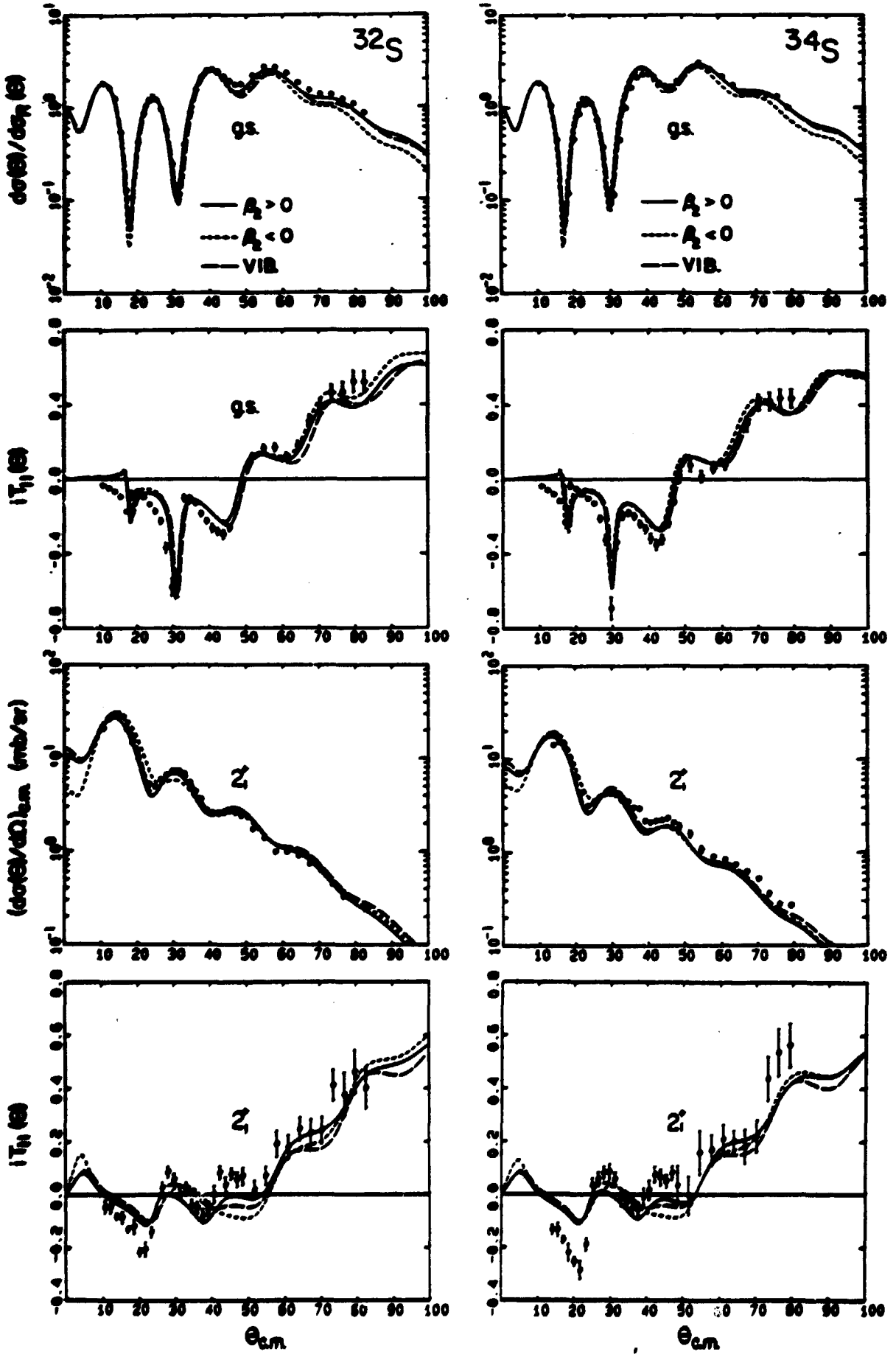
32S
34S
g.s.
$A_2 > 0$
$A_2 < 0$
VIB.
$\theta_{c.m.}$

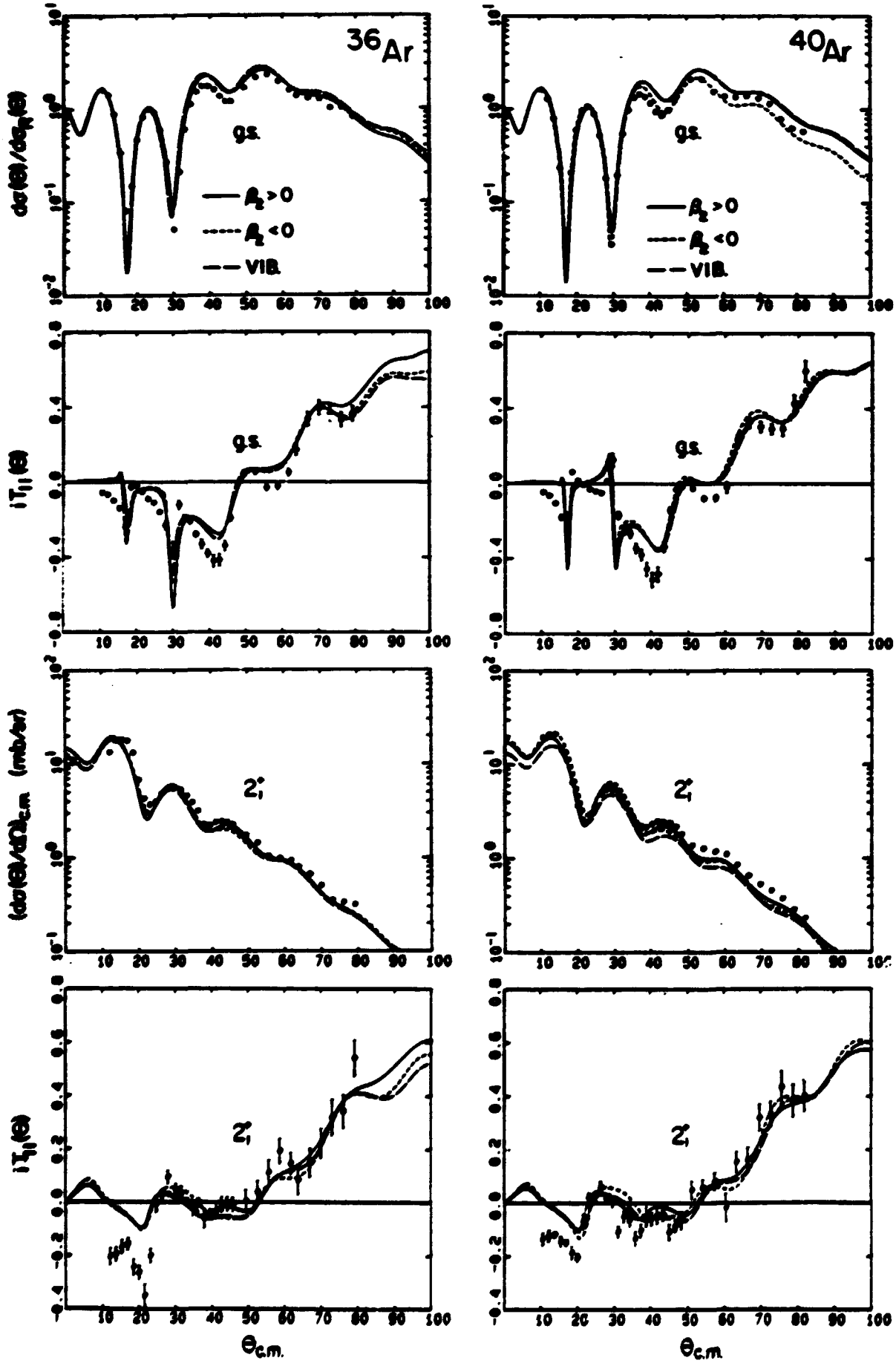
36Ar
40Ar
g.s.
$A_2>0$
$A_2<0$
VIB.
2_1^+
$\theta_{c.m.}$

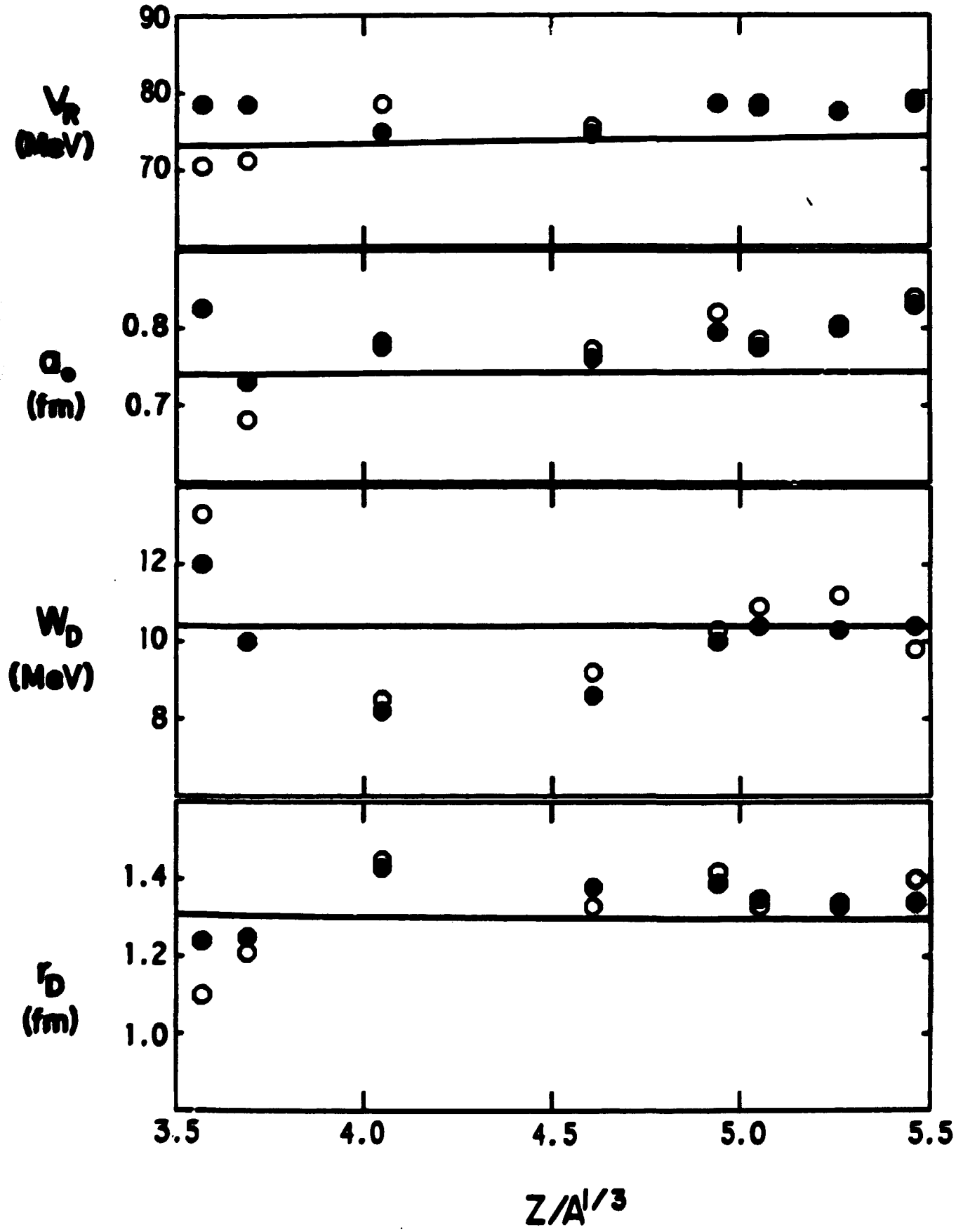
90
80
70
V_R (MeV)
0.8
0.7
a_o (fm)
12
10
8
W_D (MeV)
1.4
1.2
1.0
r_D (fm)
3.5
4.0
4.5
5.0
5.5
$Z/A^{1/3}$

Figure 6